SIMULATIONS OF FAST X-RAY DETECTORS BASED ON MULTICHANNEL PLATES *

B. Adams, Z. Insepov,# J. Norem, Argonne National Laboratory, Argonne, IL 60439, U.S.A.
V. Ivanov, Muons, Inc., Batavia, IL 60439, U.S.A.

Abstract

High-performance detectors with high spatial and time resolutions are required in applications such as imaging of fast processes, time-resolved coherent scattering, and time-resolved X-ray spectroscopy. Recently a new type of X-ray detector was proposed, based on microchannel plates (MCP) coated with resistive and emissive layers inside the pores by using atomic-layer deposition with better functional optimizations. Two microscopic Monte Carlo codes were used to calculate the characteristics of secondary electrons emitted from a photocathode irradiated by X-rays with energies of 1–15 keV and by electrons with energies in the interval of 0– -2 keV. WO_3 was selected as the photocathode and the electron emissive material. The emissive characteristics obtained by the microscopic Monte Carlo codes were used as input data for a third, macroscopic MCP simulation Monte Carlo code, for calculating the gain and transit time spread of a MCP-based X-ray detector. Our simulation results showed that the X-ray detector should improve the spatial and time resolution and push the development of high-quantum-yield photocathodes based on MCPs.

INTRODUCTION

Synchrotron-radiation science has an increasing demand for high-performance detectors with both spatial and time resolution for applications such as imaging of fast processes, time-resolved coherent scattering, and time-resolved X-ray spectroscopy. Recent developments in microchannel plate (MCP) technology hold great promise for applications in fast (sub-*ns*) and two-dimensionally spatially resolving X-ray detection.

A microchannel plate is a porous disk cut out of a bundle of hollow glass fibers that can amplify currents inside the pores through the process of cascaded secondary-electron generation. The pores are, typically, 5 to 50 microns in diameter and 40 to 60 times as long. MCPs are well established as amplifiers in imaging-type photon-detection applications, and they have also been used as efficient X-ray photocathodes [1,2].

Traditionally, MCPs are made of a type of lead glass that is chosen as a compromise of structural integrity, electrical conductivity for charge replenishment, and secondary-electron yield. Recent advances in the technology of atomic-layer deposition have now made it possible to optimize these functions separately, yielding a higher-performance, more durable, and less expensive device. ALD permits conformal and uniform thin-film coating of complicated surfaces with functional layers, such as the walls of pores in an MCP.

*Work supported by the U.S. Department of Energy under Contract No. DE-AC02-06CH11357. #insepov@anl.gov

In order to produce an MCP, ALD is used on an inexpensive porous disk cut from a borosilicate-glass fiber bundle to first lay down an electrically conductive

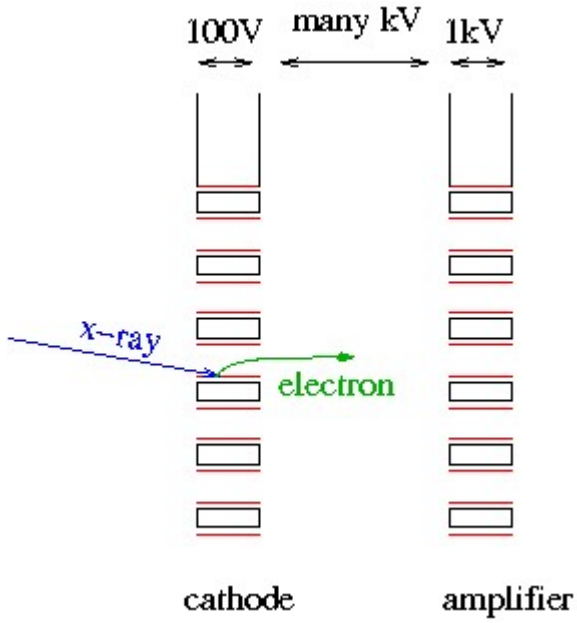

Figure 1: Layout of MCP-based photodetector.

layer (typically doped ZnO) and then a secondary-electron emitter layer (typically Al_2O_3 or MgO).

A photon detector consists of a photocathode, a stack of MCPs for amplification, and charge-collection electrodes. X-rays can be detected by using a scintillator with a visible-light photon detector or a direct-conversion photocathode. The time response of scintillators is fundamentally limited by the optical-transition oscillator strengths and is no faster than about 0.5 ns;. Moreover, the efficiency of direct conversion suffers from a mismatch of X-ray penetration and electron escape lengths. A solution to the latter problem is to operate a direct-conversion photocathode in grazing-incidence geometry. In order to do so with a large active detector area, a microchannel plate is used with the insides of the pores coated with a material that has a high X-ray stopping power (WO_3). For extracting the electrons from this MCP, a few hundred volts is sufficient, which is much lower than that required for MCP gain. This voltage can be reached with standard GHz-class RF technology, making ultrafast gating at high repetition rates possible (see Figs. 1 and 2 for details). Sub-nanosecond gain gating by launching a high-voltage pulse along a microwave strip line on the MCP surface has been demonstrated in [2]. These pulses can be generated with state-of-the-art broadband, high-power RF technology.

ISBN 978-3-95450-115-1

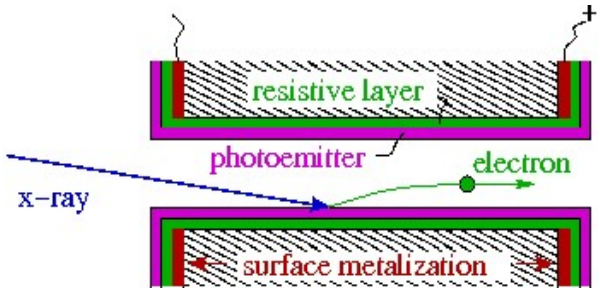

Figure 2: Resistive and emissive layers inside a pore.

The emission can be gated on or off. For high-contrast off-gating, the emission can even be reversed onto a dump electrode to suppress the prompt pulse in time-domain nuclear-resonance spectroscopy.

MC SIMULATION OF X-RAY PHOTO-EMISSION

In the photon energy range from 50 eV up to 1 GeV, the dominant interaction processes are coherent (Rayleigh) scattering, incoherent (Compton) scattering, the photoelectric effect, and electron-positron pair production. Other interactions, such as photonuclear absorption, can be neglected for most practical purposes [3].

Quantum efficiencies of photo-cathode materials were calculated by a Penelope package [3-5]. To reduce the amount of required numerical information, in Penelope, a combination of analytical differential cross-sections (DCSs) and numerical tables of total cross sections is used [3]. Further, the experimental ionization energies used were those given by Lederer and Shirley [5], which are relevant to free atoms.

The cross sections for photoelectric effect used in Penelope were obtained from the LLNL Evaluated Photon Data Library (EPDL; [6]). These data are accurate to within a few percent for photon energies above 1 keV. Since these cross sections are based on free-atom theoretical calculations, near-edge absorption structures are ignored. For mixtures and compounds, the molecular cross section is assumed to be in additive approximation, as the sum of the atomic cross sections.

Theory of QE in WO_3

Along the line of photon propagation, high-energy primary electrons are emitted that are either emitted from the pore surface or captured by a cascade of electron-electron collisions inside the material via ionization. The primary energetic electrons will still be absorbed inside the pore and therefore, we assume they do not contribute to the gain. The secondary electrons have low energies not sufficient to overcome the surface barrier and they have a diffusive characteristic length L. The quantum efficiency of a photocathode can be estimated by the total number of emitted secondary electrons per second, n_{SE}, to the total number absorbed photons, n_{ph}.

$$QE = n_{SE}/n_{ph} \qquad (1)$$

The QE formula can be obtained by assuming that the total energy of an X-photon is shared between many slowly diffusing secondary electrons from a point source [7]:

$$QE = \Delta K(\phi)\cdot\left[1 - R(\phi)\right]\frac{\hbar\omega}{\varepsilon} B \frac{\mu' L}{1+\mu' L}, \qquad (2)$$

where L is the diffusion length of secondary electrons that was calculated to be in the interval L = 10–100 nm, depending on the WO_3 film quality, B = 0.5–1.0 is the probability of escaping through the surface, μ' is the X-ray mass coefficient of absorption that was calculated by the Penelope MC code in this paper, ε = 8.6 eV, and by an empirical formula obtained in [7], and the result is shown in Fig. 3. $\Delta K \approx 10^{-3}$ [9,10]. Figure 3 shows QE calculated by Eq. (2) for four diffusion lengths L=100–910 Å, where the mass absorption coefficients were obtained by the Penelope code calculations.

Monte Carlo Calculation of SEE Yield for WO_3

The SEE yield is obtained by a Monte Carlo (MC) code that was developed by D. Joy [9,10] and were applied to Al_2O_3 and MgO in our previous paper [11]. The MC model has two important simulation parameters. One is ε, the average energy for producing secondary electron, and the other is the escape depth λ. We used ε = 20 eV for WO_3. The escape depth λ of insulators can be relatively large compared with metal surfaces, which is a direct effect of the small absorption coefficient of low energy electrons in insulators because of the large energy band gap (e.g. E_g = 2.75 eV in WO_3)[12]. Kanaya et al. [13] proposed a theoretical model that allows one to calculate the escape depth for a range of insulators and alkaline materials. Based on this analysis, the escape length has been chosen to be in the interval λ = 100–1000 Å for WO_3. Fig. 4 shows the primary electron energy and angular dependences of the secondary electron emission (SEE) yields of WO_3 calculated by MC code.

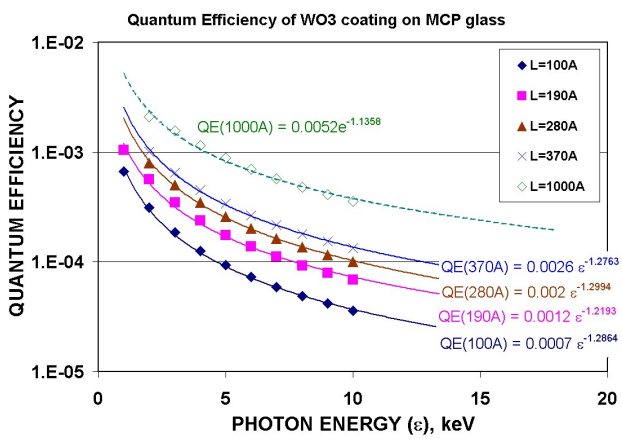

Figure 3: Photon linear attenuation coefficient calculated by Penelope (diamonds) and by empirical model developed in [8] (squares).

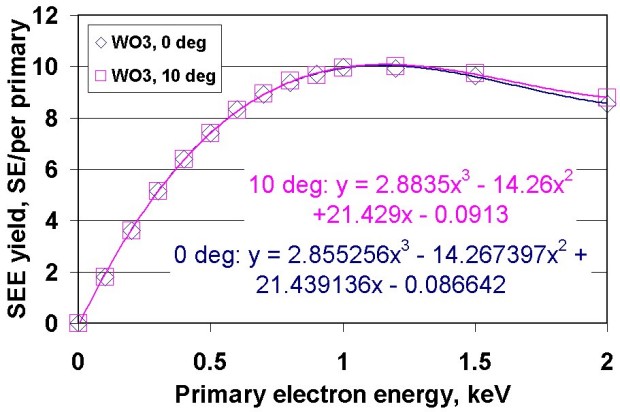

Figure 4: Primary electron energy and angular dependences (for clarity, the results for larger angles, 20°-80°, are not shown) of the secondary electron emission (SEE) yields of WO_3 : thickness 100 nm, electron escape length λ = 100 nm, obtained by the MC calculations.

MC Calculations of Gain and TTS for the MCP-Based Photo-Detector

The original code "MCS" [11] was used to provide the modelling of a large-area X-ray imaging detector in 3D. Here the photons of 10 KeV energy illuminate the MCP pore surface with a random position during the pulse time, and produce the primary electrons with probability QE, Lambert's angular and Chung-Everhart's energy distributions.

Figs. 5 and 6 show our calculated results for the gain dependence on the applied MCP voltage for different SEE-yield curves and a pulse-shape profile of the current density on time predicted for the future photo-detector based on MCP coated with WO_3.

Those electrons propagate in the electric field within the pore, hit the wall, and create the cascades of secondary electrons. Actually Fig. 4 shows the SEE yield from an ideal polycrystalline WO_3. The real material can have lower yield, so the calculations for different dependencies characterized by a σ_{max} values were done.

Numerical simulations are reliable instruments to understand the physical processes in the MCP pores, and to optimize the work modes of modern photo detectors.

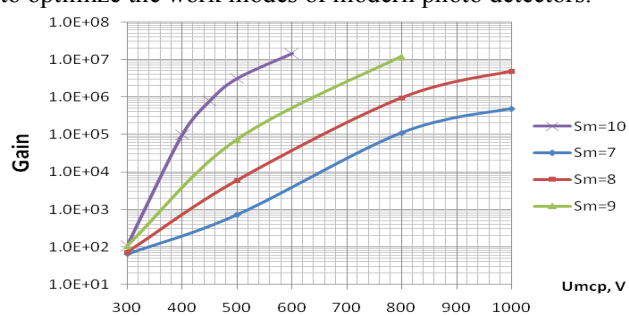

Figure 5: The gain vs. applied MCP voltage for different SEE-yield curves.

Acknowledgment: This work was supported by the U.S. Department of Energy, Office of Basic Energy Sciences under Contract No. DE-AC02-06CH11357 .

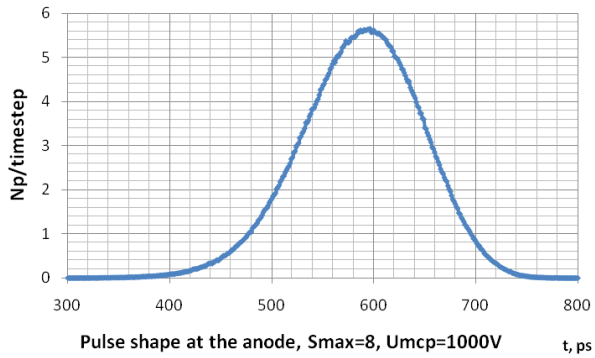

Figure 6: Pulse-shape profile shows the current density vs. time.

REFERENCES

[1] G. A. Rochau et al., Rev. Sci. Instr. **77** (2006) 10E323.
[2] M. Katayama et al., Rev. Sci. Instr. **62** (1992) 124-129.
[3] F. Salvat, J.M. Fernández-Varea, J. Sempau, Penelope, A code system for Monte Carlo simulation of electron and photon transport, AEN-NEA, 2006.
[4] R.H. Pratt, A. Ron and H.K. Tseng, Rev. Mod. Phys. 45, 273–325.
[5] C.M. Lederer, V.S. Shirley, eds., Table of Isotopes, 7th ed. Wiley, New York, 1978.
[6] D.E. Cullen, J.H. Hubbell, L. Kissel (1997), Report UCRL-50400, vol. 6, rev. 5, Lawrence Livermore National Laboratory, Livermore, CA.
[7] V.N. Shemelev, E.P. Savinov, Solid St. Phys., 40(6), 1042–1046.
[8] J. A. Victoreen, J. Appl. Phys. 20 (1949) 1141-1147.
[9] D.C. Joy, Monte Carlo Modeling for Electron Microscopy and Microanalysis, Oxford University Press, 1995.
[10] D.C. Joy, A model for calculating secondary and backscattering electron yields, J. Microscopy, 147, 51–64 (1987).
[11] Z. Insepov, V. Ivanov, S.J. Jokela, I. Veryovkin, A. Zinovev, H. Frisch, Nucl. Instr. and Meth. in Phys. Res. A 639, 155-157 (2011).
[12] P. P. González-Borrero, F. Sato, A. N. Medina, M. L. Baesso, A. C. Bento et al., Appl. Phys. Lett., 96, 061909 (2010).
[13] K. Kanaya, S. Ono, F. Ishigaki, J. Phys. D: Appl. Phys., 11, 1978.

ISBN 978-3-95450-115-1